Osteoarthritis and Cartilage 27 (2019) 1235–1243

Osteoarthritis and Cartilage

Near-infrared spectroscopy enables quantitative evaluation of human cartilage biomechanical properties during arthroscopy

M. Prakash † ‡ *, A. Joukainen §, J. Torniainen † ‡, M.K.M. Honkanen † ‡, L. Rieppo † ‖, I.O. Afara †, H. Kröger §, J. Töyräs † ‡ ¶, J.K. Sarin † ‡

† *Department of Applied Physics, University of Eastern Finland, Finland*
‡ *Diagnostic Imaging Center, Kuopio University Hospital, Kuopio, Finland*
§ *Department of Orthopedics, Traumatology and Hand Surgery, Kuopio University Hospital, Kuopio, Finland*
‖ *Research Unit of Medical Imaging, Physics and Technology, Faculty of Medicine, University of Oulu, Oulu, Finland*
¶ *School of Information Technology and Electrical Engineering, The University of Queensland, Brisbane, Australia*

ARTICLE INFO

Article history:
Received 24 October 2018
Accepted 9 April 2019

Keywords:
Articular cartilage
Near-infrared (NIR) spectroscopy
Human knee joint
Principal components
Arthroscopy
Statistical decision making
Machine learning

SUMMARY

Objective: To investigate the feasibility of near-infrared (NIR) spectroscopy (NIRS) for evaluation of human articular cartilage biomechanical properties during arthroscopy.
Design: A novel arthroscopic NIRS probe designed in our research group was utilized by an experienced orthopedic surgeon to measure NIR spectra from articular cartilage of human cadaver knee joints (*ex vivo*, $n = 18$) at several measurement locations during an arthroscopic surgery. Osteochondral samples ($n = 265$) were extracted from the measurement sites for reference analysis. NIR spectra were remeasured in a controlled laboratory environment (*in vitro*), after which the corresponding cartilage thickness and biomechanical properties were determined. Hybrid multivariate regression models based on principal component analysis and linear mixed effects modeling (PCA-LME) were utilized to relate cartilage *in vitro* spectra and biomechanical properties, as well as to account for the spatial dependency. Additionally, a k-nearest neighbors (kNN) classifier was employed to reject outlying *ex vivo* NIR spectra resulting from a non-optimal probe-cartilage contact. Model performance was evaluated for both *in vitro* and *ex vivo* NIR spectra via Spearman's rank correlation (ρ) and the ratio of performance to interquartile range (RPIQ).
Results: Regression models accurately predicted cartilage thickness and biomechanical properties from *in vitro* NIR spectra (Model: $0.77 \leq \rho \leq 0.87$, $2.03 \leq \text{RPIQ} \leq 3.0$; Validation: $0.74 \leq \rho \leq 0.84$, $1.87 \leq \text{RPIQ} \leq 2.90$). When predicting cartilage properties from *ex vivo* NIR spectra ($0.33 \leq \rho \leq 0.57$ and $1.02 \leq \text{RPIQ} \leq 2.14$), a kNN classifier enhanced the accuracy of predictions ($0.52 \leq \rho \leq 0.87$ and $1.06 \leq \text{RPIQ} \leq 1.88$).
Conclusion: Arthroscopic NIRS could substantially enhance identification of damaged cartilage by enabling quantitative evaluation of cartilage biomechanical properties. The results demonstrate the capacity of NIRS in clinical applications.

Introduction

Articular cartilage is a thin layer of connective tissue lining the ends of articulating bones. This specialized tissue enables near-frictionless movement of the joint and distributes stress to the underlying bones. Mature articular cartilage can be divided into three layers, namely, superficial, middle, and deep zones. Collagen type II, proteoglycans (PGs), chondrocytes, and water are the primary constituents of cartilage and the amount of these constituents varies between zones[1]. Cartilage biomechanical properties are primarily influenced by the interplay of collagen orientation, PG

* Address correspondence and reprint requests to: M. Prakash, Department of Applied Physics, University of Eastern Finland, Kuopio, Finland. Tel: 358-449207680.
E-mail addresses: mithilesh.prakash@uef.fi (M. Prakash), antti.joukainen@kuh.fi (A. Joukainen), jari.torniainen@uef.fi (J. Torniainen), miitu.honkanen@uef.fi (M.K.M. Honkanen), lassi.rieppo@oulu.fi (L. Rieppo), isaac.afara@uef.fi (I.O. Afara), heikki.kroger@kuh.fi (H. Kröger), juha.toyras@uef.fi (J. Töyräs), jaakko.sarin@uef.fi (J.K. Sarin).

https://doi.org/10.1016/j.joca.2019.04.008
1063-4584/

distribution, and cartilage permeability[2,3]. Collagen network is mainly responsible for dynamic compressive stiffness while the PGs control static mechanical properties[4–6]. The mechanical properties of articular cartilage can be experimentally determined with indentation testing which measures the load response of the tissue[7,8]. Alterations in any of cartilage constituents can lead to its mechanical failure and in turn, lead to impaired joint function or even osteoarthritis (OA).

Post-traumatic osteoarthritis (PTOA) is a joint disease often initiated by excessive loading conditions, such as accidental falls or sports injuries[9]. Unlike other joint tissues, articular cartilage is avascular and aneural; hence, it has limited self-healing properties[10,11]. Biomechanical properties of healthy and damaged cartilage differ substantially and are therefore good indicators of tissue health[3]. Currently, arthroscopic diagnostics of cartilage injuries and degeneration relies on visual evaluation and manual palpation of the cartilage surface with a metallic hook[12]. These methods are highly subjective and only enable evaluation of cartilage surface[13], thus necessitating more robust, quantitative, and reliable alternatives[14,15].

Analytical vibrational spectroscopy methods, such as Raman, mid-infrared (MIR), and near-infrared (NIR) spectroscopy, have been utilized to quantify the properties of cartilage[16]. These methods are used to study the molecular vibrations of samples. NIR spectroscopy (NIRS) has been successfully applied for the evaluation of cartilage properties in animal models by providing a rapid characterization (*i.e.*, between healthy and damaged) and mapping of tissue properties[17,18]. To relate complex NIR spectra and tissue properties, multivariate analysis is required[19].

Conventional multivariate regression techniques, such as partial least squares (PLS), have been successful in relating optical data to cartilage properties but face limitations and are potentially unreliable in experimental scenarios[19], such as mapping tissue properties in arthroscopy, where adjacent measurement locations (repeated measures) violate the assumption of independent observations[20,21]. These limitations of the conventional regression techniques were addressed by Prakash *et al.*[22], where a viable solution based on a hybrid multivariate regression technique was proposed to overcome these limitations. Another limitation to the arthroscopic application of NIRS is associated with the poor accessibility to cartilage surfaces due to the narrow joint space[23]. This limited access may result in suboptimal probe alignment and, thus, impact the spectral acquisition. This limitation needs to be addressed during the analysis.

We hypothesize that by employing hybrid statistical regression models, we can reliably predict cartilage biomechanical properties from NIR spectra during knee arthroscopy. To test this hypothesis, NIR spectra were first collected from cadaveric human knee joints (*ex vivo*) arthroscopically and later in a controlled laboratory environment (*in vitro*). Regression models were developed to predict tissue properties from *in vitro* NIR spectra and subsequently validated using the arthroscopically acquired *ex vivo* data. In addition, a classifier was trained to efficiently detect noisy spectra during arthroscopy. This process will both validate the application of NIRS for clinical evaluations and result in a prediction model applicable for further *in vivo* clinical testing.

Material and methods

In this study, tibial, femoral, and patellar surfaces of both knee joints of human cadavers (n = 8 males and 1 female, Age = 68.4 ± 7.45) were arthroscopically examined by an experienced orthopedic surgeon at Kuopio University Hospital, Kuopio, Finland. First, cartilage integrity was assessed with a conventional arthroscope (4 mm, 30° inclination Karl Storz GmbH & Co, Tuttlingen, Germany) in accordance with the International Cartilage Repair Society (ICRS) grading system[24]. Next, NIR spectra (n = 15 per location, each spectrum was an average of ten successive spectra, $t_{15\ spectra}$ = 2.4 s) were acquired using a novel NIRS probe (Fig. 1). During the measurements, knee joints were distended with saline solution (25 °C, 0.9% NaCl concentration). Subsequently, osteochondral blocks were harvested and frozen (−20°C) in

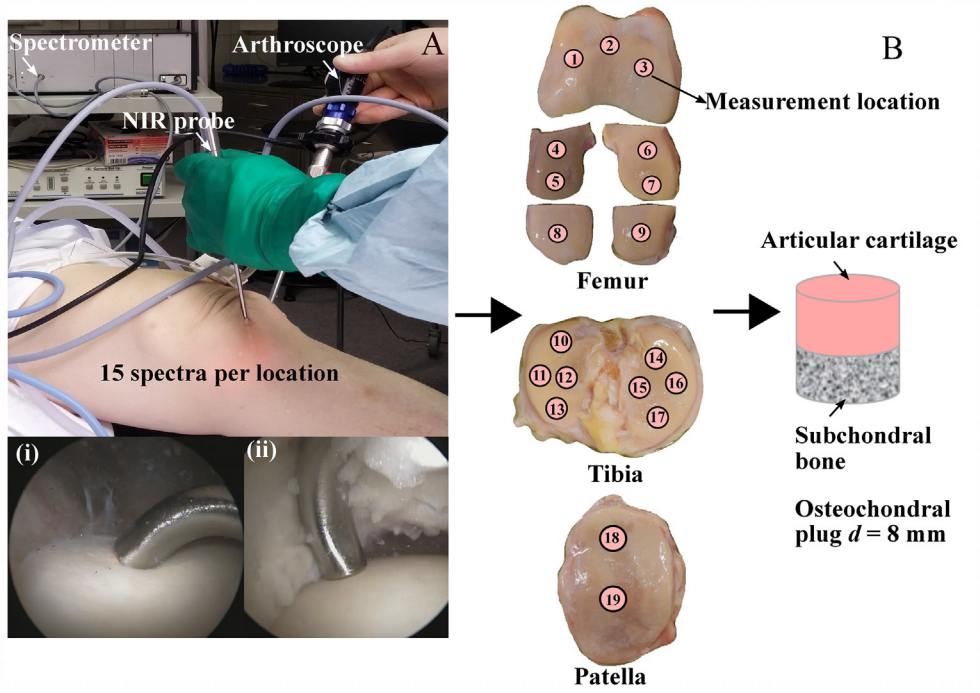

Fig. 1. A: Arthroscopic acquisition of near-infrared (NIR) spectral data from articular cartilage (*ex vivo*). The inset figures show (i) sub-optimal (not perpendicular) and (ii) optimal probe-cartilage contact as observed on the video feed. **B:** Osteochondral plugs (~19) were extracted from osteochondral blocks at locations corresponding to the NIRS measurements.

phosphate-buffered saline (PBS). To preserve the sample, PBS was complemented with proteolytic enzyme inhibitors, namely ethylenediaminetetraacetic acid disodium salt (1.86 g/L, EDTA VWR International, Radnor, PA, USA) and benzamidine hydrochloride hydrate (0.78 g/L, Sigma–Aldrich Co., St. Louis, MO, USA). During arthroscopic spectral measurements, the ICRS knee cartilage lesion mapping system, described by Brittberg *et al.*[24], was utilized to mark the measurement and sample extraction locations (Fig. 1(B)). Additionally, arthroscopic videos were recorded with an endoscopic camera to ensure that the extracted locations and measured locations coincided. The study was approved by the local research ethics committee (Decision number 150/2016, Research Ethics Committee of the Northern Savo Hospital District, Kuopio University Hospital, Kuopio, Finland).

Prior to performing NIRS measurements in a controlled environment (*in vitro*), osteochondral plugs ($d = 8$ mm, $n = 265$) were extracted after thawing the osteochondral blocks. During the NIRS measurements, the osteochondral plugs were placed on a black rubber sample holder and immersed in a saline solution. NIR spectra were acquired at the same temperature (25 °C) as the *ex vivo* measurements were conducted. After establishing optimal (perpendicular) probe contact with cartilage surface, spectral data (average of three spectra per location) was acquired.

Near-infrared spectroscopy

The main instrumentation (Fig. 1(A)) consisted of a light source (AvaLight-HAL-(S)-Mini, $\lambda = 360–2{,}500$ nm, Avantes BV), two spectrometers (AvaSpec-ULS2048L, $\lambda = 350–1{,}100$ nm, resolution = 0.6 nm and AvaSpec-NIR256-2.5-HSC, $\lambda = 1{,}000–2{,}500$ nm, resolution = 6.4 nm, Avantes BV, Apeldoorn, Netherlands), and a customized optical probe. The design of the stainless-steel probe resembles a conventional arthroscopic hook, and it can withstand autoclave sterilization process (Fig. 2). The probe ($d = 2$ mm, inner diameter) houses 114 fiber optical strands ($d = 100$ μm), with 100 strands for illuminating the sample and seven for each spectrometer to collect the diffusely reflected light from the sample (Fig. 2). During spectral measurements, perpendicular orientation between probe tip (plane-ended) and cartilage surface is required. This is to prevent spectral saturation due to absorption of NIR light in saline, which is necessary for joint irrigation. The probe was designed to collect the spectra with short acquisition time and to provide surgeons with a familiar looking tool that can be used similarly as the palpation hook (Fig. 2(A)). Further research on probe design is ongoing to ensure optimal probe-cartilage contact.

Measurements of cartilage thickness and biomechanical properties

Cartilage thickness was determined using a Vernier caliper (resolution = 0.01 mm). The thickness was estimated as the average of four longitudinal measurements equidistant around the perimeter of the plugs. Biomechanical properties of the osteochondral plugs were determined via indentation testing using a custom material testing device[5].

The material testing device consisted of a plane-ended indenter ($d = 667$ or 728 μm), a load cell (1,000 g, accuracy ± 0.25%, Model 303 31, Honeywell Sensotec Sensors, Columbus, OH, USA), and an actuator (displacement resolution 0.1 μm, PM500-1 A, Newport, Irvine, CA, USA). The osteochondral plugs were kept immersed in PBS containing inhibitors of proteolytic enzymes throughout the biomechanical measurements.

The biomechanical protocol consisted of stress–strain relaxation and sinusoidal measurements. To ensure good contact between cartilage and indenter, 12.5 kPa pre-stress was established, followed by five preconditioning cycles (2% strain)[8]. Subsequently, a 3-step mechanical testing protocol (5% of remaining cartilage thickness at each step with 100%/s ramp rate) was applied with the relaxation time between each step being 900 s. Instantaneous modulus (E_{ins}) was determined at the ramp phase of the 3rd step and equilibrium modulus (E_{eq}) from the fit to the last three equilibrium points. Subsequently, sinusoidal loading (4 cycles, 1 Hz, 2% strain amplitude) was applied to determine dynamic modulus (E_{dyn} = ratio of the stress and strain amplitudes). Moduli were

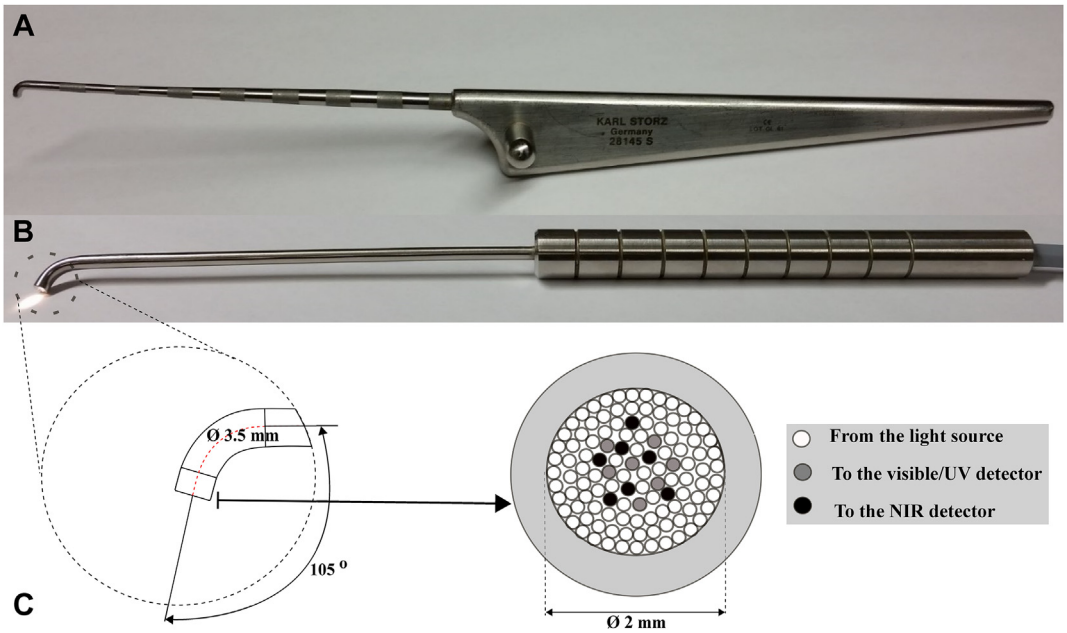

Fig. 2. A conventional arthroscopic hook (A) used by orthopedic surgeons and the NIRS probe (B) designed by our research group (Biophysics of Bone and Cartilage, Kuopio, Finland). A schematic diagram (C) of the probe tip and the arrangement of optical fibers is provided.

computed using the Hayes solution assuming Poisson ratio of $\nu = 0.5$, 0.1, and 0.5 for E_{ins}, E_{eq}, and E_{dyn}, respectively[25]. During the measurements, two indenters were used as one got damaged. The effect of using two slightly different indenters on the measured biomechanical response of the tissue is minimal, as this was taken into account during the calculation of the biomechanical parameters.

Spectral preprocessing

A 3rd order Savitzky–Golay filter was utilized for smoothing the spectral data. The spectral data from both spectrometers (AvaSpec-ULS2048L and AvaSpec-NIR256-2.5-HSC) were processed separately with different smoothing window sizes (29 data points [17.40 nm], 17 data points [108.8 nm]) due to different resolutions[25]. Spectral data covering the region 710–1,850 nm was utilized in the analysis as the visible spectral region (400–710 nm) had contributions from the light source of conventional arthroscope. Additionally, spectral regions 1,350–1,450 nm and 1,850–2,500 nm were excluded from analysis due to the pronounced effect of water (saturation of the signal). The mean coefficient of variation of NIR signal acquired during arthroscopies was 2.35 ± 2.94%.

Regression analysis

Adjacent measurement locations (Fig. 1) are spatially dependent and hence, we employed principal component analysis-based linear mixed effects regression (PCA-LME) to predict cartilage biomechanical properties from its NIR spectral data[22]. PCA reduces the high dimensionality of the NIR spectra and provides scores as input to the regression model, while LME accommodates the nested data, *e.g.*, samples from each knee and knees from each subject (Fig. 3). PCA-LME was chosen for its computational simplicity and performance consistency over LASSO (least absolute shrinkage and selection operator)-LME[22]. In model calibration, PCA-LME can accommodate dependency levels which include grouping information of the measurement locations. These dependency levels need to be accounted for in order to fulfill the assumptions of independent observations[21].

The measurement locations (n = 19, Fig. 1), bones of the knee joint (n = 3, tibia, femur and patella), joint level grouping (n = 2, left or right knee), and cadaver level grouping (n = 9) are identified as the most relevant dependency levels[26]. Design matrix (number of samples × number of levels) was created to hold the grouping information needed for PCA-LME. The resulting LME equation (Equation (1)) consists of accommodated dependency levels (1| dependency level) as mixed effects and dimension reduced NIR spectra via PCA scores as fixed effects.

$$\begin{aligned}\text{Tissue property} \sim\ & \text{PCA scores} + (1|\text{Location}_{1-19}) \\ & + (1|\text{Bones}_{\textit{Tibia, Femur\& Patella}}) \\ & + (1|\text{Joints}_{\textit{Left, Right}}) + (1|\text{Cadaver}_{1-9})\end{aligned} \tag{1}$$

In vitro models were calibrated and optimized (for details readers are referred to Prakash *et al.*[22]) on data from 16 joints (8 cadavers) by utilizing 10-fold cross-validation. The performance of the calibrated models was validated using the remaining cadaver (test group). The calibration and test groups were cycled through nine iterations with each cadaver used once as a test group. Hence, PCA-LME prediction models were calibrated on a wide range of tissue properties covering both healthy (ICRS 0 and 1, Table I) and degraded locations (ICRS 2 and 3, Table I).

The kNN classifier for rejecting spectra with bad probe-cartilage contact

During arthroscopic NIR spectral acquisition, optimal contact between the probe and cartilage surface may not always be possible (Fig. 1(i)). As a non-optimal probe-cartilage contact may result in the unreliable spectral acquisition and hence poor prediction performance, it is necessary to exclude the spectral outliers. Therefore, a classifier is required to retain ('good') spectra with optimal contact and reject ('bad') spectra with poor contact.

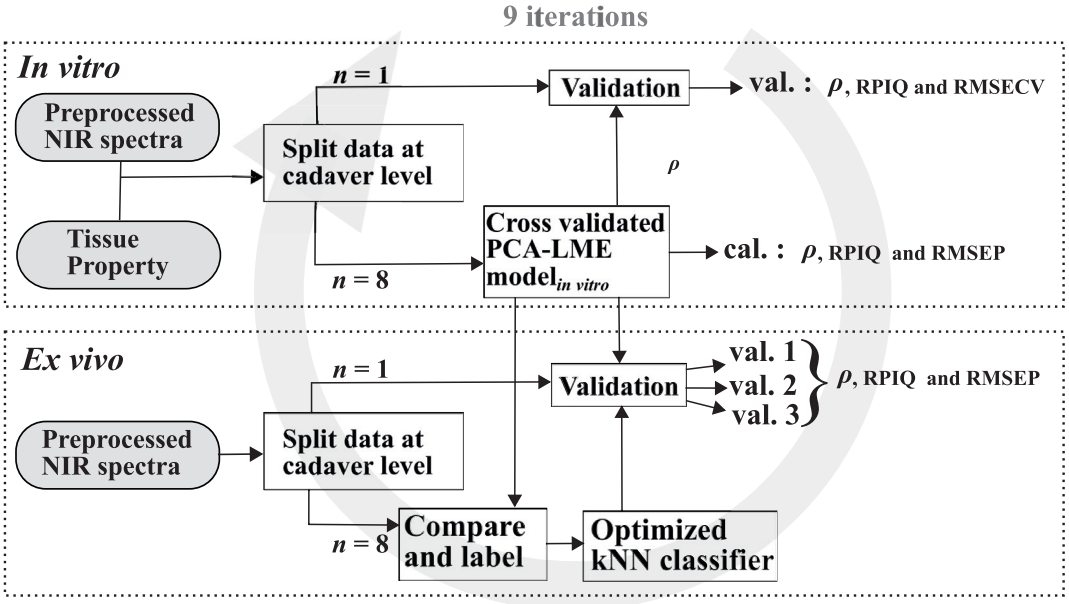

Fig. 3. A schematic showing the process flow of the PCA-LME regression modeling and a kNN filter.

Table I
A summary of tissue properties of both knees of each cadaver. The mean (range) values of International Cartilage Repair Society (ICRS) grade, thickness, and biomechanical parameters are presented.

Cadaver number	Number of measurement locations	ICRS grade	Thickness (mm)	Instantaneous modulus (MPa)	Equilibrium modulus (MPa)	Dynamic modulus (MPa)
1	30	1.04 (0–3)	2.94 (1.86–5.90)	15.27 (1.08–41.98)	1.10 (0.09–3.23)	6.39 (0.62–16.08)
2	29	1.04 (0–2)	2.67 (1.46–4.69)	12.64 (0.39–30.91)	1.12 (0.04–3.68)	5.77 (0.24–13.57)
3	25	2.45 (1–4)	2.29 (1.33–3.31)	11.57 (0.52–51.82)	0.61 (0.03–2.03)	4.90 (0.34–18.00)
4	25	1.97 (0–4)	2.55 (1.23–4.59)	11.77 (0.20–33.77)	0.58 (0.03–1.55)	4.38 (0.14–10.36)
5	32	1.77 (0–3)	2.59 (1.24–3.90)	12.04 (0.13–32.48)	0.80 (0.02–2.31)	4.84 (0.10–12.55)
6	30	1.14 (0–3)	2.51 (1.52–3.58)	10.67 (1.04–30.16)	0.42 (0.04–1.14)	3.64 (0.49–09.07)
7	24	0.73 (0–3)	2.51 (1.76–4.62)	16.38 (0.24–48.40)	1.24 (0.02–2.88)	6.79 (0.14–19.76)
8	33	1.54 (0–4)	2.36 (1.35–4.04)	13.24 (1.05–34.78)	0.85 (0.04–3.12)	5.29 (0.58–14.12)
9	33	1.00 (0–3)	2.78 (1.75–4.01)	20.04 (0.96–44.82)	1.25 (0.06–2.68)	7.63 (0.48–16.76)

First, the trained *in vitro* PCA-LME model was used to predict cartilage properties from *ex vivo* spectra (Fig. 3). Next, the deviations between the predicted and measured values were calculated. If the deviation was higher than the calibration error (mean squared error) of the *in vitro* PCA-LME model, the spectrum was rejected and labeled as 'bad'. Subsequently, a k-nearest neighbors (kNN) classifier was trained using PCA scores of *ex vivo* spectra from the calibration dataset (16 joints, same as used for the *in vitro* model training) and their corresponding labels[27]. The classifier was optimized through a 25% holdout. Finally, the trained kNN classifier was utilized to retain or reject arthroscopic spectra from the independent testing group (2 joints). The retained ('good') spectra from each location were averaged and the tissue properties predicted using the *in vitro* model.

Statistical analyses

The usage of coefficients of determinations (R^2) for linear mixed effects models is unclear and hence Spearman's rank correlation (ρ) was chosen as a distribution independent and a nonparametric statistic[22,28,29]. Additionally, to evaluate model performance and reliability, the ratio of performance to interquartile range (RPIQ) was computed[30]. RPIQ is computed as a ratio of root mean square error (RMSE) to interquartile range. RPIQ was chosen due to non-normal data distribution. Based on previous studies for an acceptable model, the RPIQ value should fall between 1.5 to 3.0[23,31]. MATLAB R2018b (The Mathworks Inc, Natick, MA) was utilized for implementing algorithms and analysis.

Results

Hybrid regression models (PCA-LME) predicted cartilage thickness and biomechanical properties (Table I) from *in vitro* NIR spectra with good accuracy (Model: $0.77 \leq \rho \leq 0.87$, $2.03 \leq \text{RPIQ} \leq 3.0$; Validation: $0.74 \leq \rho \leq 0.84$, $1.87 \leq \text{RPIQ} \leq 2.90$, Figs. 4 and 5). Predictions of cartilage properties with *in vitro* models from *ex vivo* NIR spectra ($0.52 \leq \rho \leq 0.87$ and $1.06 \leq \text{RPIQ} \leq 1.88$) were aided by a kNN classifier (accuracy: 50–70% in identifying the labels of the holdout data). Without the classifier rejecting 'bad' spectra, the performance was poor ($0.33 \leq \rho \leq 0.57$ and $1.02 \leq \text{RPIQ} \leq 2.14$). In the test set, the classifier sometimes retained or rejected all 15 spectra but on an average 5 out of 15 spectra were rejected (Fig. 6). Comparison of val.2 and val.3 (Fig. 4) shows that the classifier is effective for rejecting acquisitions involving probe misalignment and 'bad' spectrum. Due to the nonparametric classification nature of the kNN filter, the features of excluded spectra are not easily identified. However, observations (Fig. 6) on the mean spectra suggest that the mean of rejected spectra has a larger deviation from the mean *in vitro* spectra in comparison to the deviation from the mean of selected spectra. The possible influence of detector saturation in the 1,350–1,450 nm and 1,850–2,500 nm regions due to water between probe and cartilage was minimized by excluding these water peaks from the analysis.

Discussion

In this study, for the first time, human cartilage thickness and biomechanical properties were predicted from NIR spectra acquired during *ex vivo* arthroscopy. Furthermore, no previous study has utilized a combination of a spectral classifier and a hybrid regression technique to reject spectral outliers and to account for sample dependency, respectively. In practice, surgeons rely on manual palpation and visual evaluation of cartilage to assess its condition during arthroscopy[12]. These methods only enable subjective and superficial evaluation[32]. Furthermore, existing underlying chondral damage may go undetected as the surface appears intact. Our study demonstrates the applicability of NIRS for arthroscopies and that the technique could substantially enhance the detection of cartilage degeneration.

Although NIRS has been previously applied for arthroscopic evaluation of human joints[33,34], these studies employed univariate regression methods based on absorptions of two spectral peaks (*i.e.*, 1,150–1,220 nm and 1,340–1,475 nm) for diagnostic assessment of cartilage condition. In the present study, a hybrid multivariate technique was utilized, taking advantage of the multi-wavelength relationship with cartilage properties accessible from broadband spectra[19]. Furthermore, spatial dependency, which is a common limitation of clinical studies due to multiple adjacent measurement locations, was accounted for via the hybrid regression models[21,22].

Several studies have demonstrated the relationship between absorption spectra and cartilage biomechanical properties and thickness[23,35–37]. These studies are mostly based on animal models, except for Afara *et al.*[37], that utilized cadaveric tissue *in vitro*. However, they acquired no arthroscopic spectra and they also utilized a narrower spectral region (750 to 1,100 nm) compared to this study[37]. The arthroscopic approach provides more information for *in vivo* NIRS assessment of cartilage properties in human patients, specifically in identification of the extent of post-traumatic degeneration around the chondral lesion, similar to a recent application in equine samples[23]. The *in vitro* PCA-LME model's correlations (*thickness* = 0.80, $E_{eq} = 0.70$, $E_{dyn} = 0.78$) are similar or higher when compared to previously reported findings (Afara *et al.*[35]: *thickness* = ~0.84; Marticke *et al.*[36], $E_{eq} = 0.53$). Similarly, our arthroscopic results ($E_{eq} = 0.70$, $E_{dyn} = 0.65$) agrees with the findings of Sarin *et al.* ($E_{eq} = 0.59$, $E_{dyn} = 0.61$)[23].

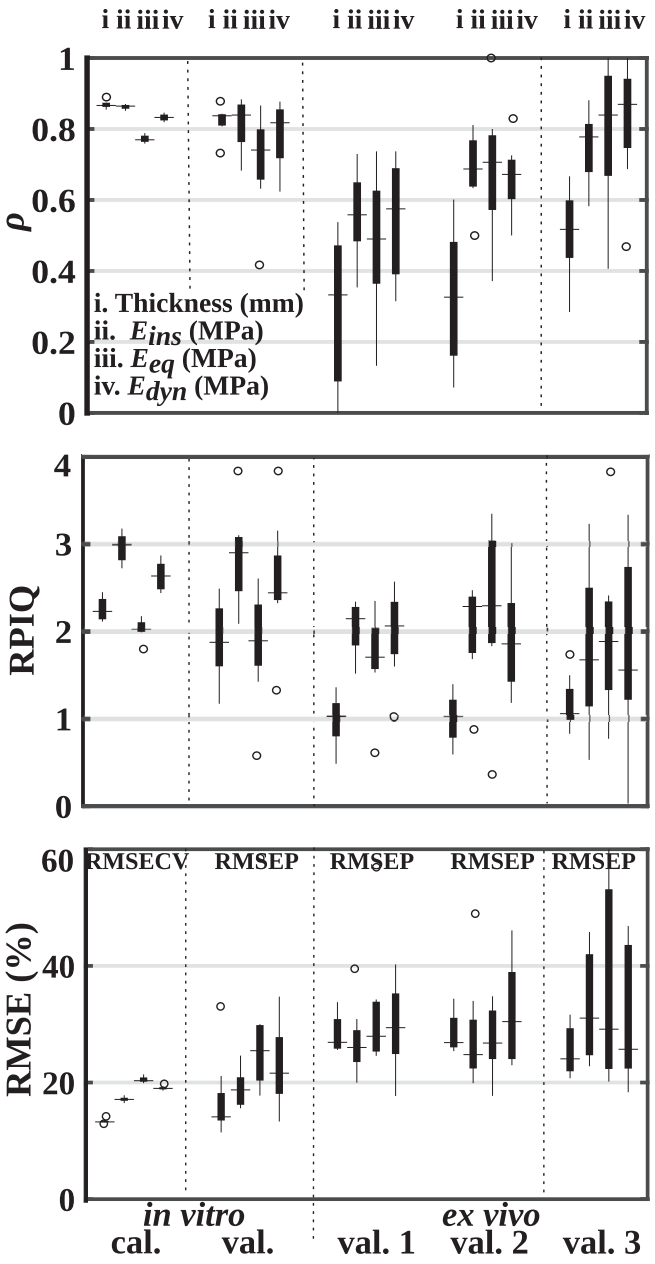

Fig. 4. Boxplots of PCA-LME model performance in terms of Spearman's correlation coefficient (ρ), ratio of performance to interquartile range (RPIQ), and root mean square error (RMSE) of cross-validation (RMSECV) and prediction (RMSEP) of all model iterations ($n = 9$). The calibration (cal.) and validation (val.) for *in vitro*, and validation performance of the arthroscopies (*ex vivo*) without classifier (val. 1) and with classifier (val. 3) are shown. In group val. 2, the locations with all 'bad' spectra were excluded from val. 1; thus, groups val. 2 and val. 3 had the same number of measurement locations. The horizontal line on the quartiles (25–75%) indicates the median of the distribution.

The correlations observed in our models arise from overtone vibrations of O–H, N–H and C–H chemical bonds which are the most abundant bonds of cartilage constituents (*i.e.*, water, PGs, and type II collagen)[38]. The strong correlation between NIR absorbance values and cartilage thickness was observed with the *in vitro* model due to the contribution of path length on light absorption and the reflection from the interface of cartilage and subchondral bone[35,39]. However, predicting cartilage thickness from *ex vivo* spectra had higher errors, arguably due to variation in the quantity of reflected light from the cartilage–bone interface and possibly due to the variation in contact pressure of the probe on cartilage surface which could potentially alter the optical properties of the tissue and thus the spectra[35,40–42]. Furthermore, spectra acquired with wider spectral region (400-1,900 nm) may include interactions from the subchondral bone[39]. This constraint could affect the prediction of cartilage thickness but is outside the scope of the current study. Thus, arthroscopic measurement protocol requires further optimization to improve the prediction of cartilage thickness. The prediction of biomechanical parameters was more reliable than predicting cartilage thickness. Most probably the spectral response from the superficial cartilage layer, which substantially contributes to cartilage biomechanical capacity, is sufficient for accurate prediction of biomechanical properties. Although spectral region could be restricted to 1,400–2,500 nm, as per Padalkar *et al.*[39], to limit the effects of subchondral bone[43], the benefits of utilizing wider spectral region in terms of improved correlation with biomechanical properties and compositional properties outweigh its cons[23,44].

In an earlier comparative study, PLS regression (PLSR) was found to be an optimal regression method for NIRS-based characterization of cartilage properties[19]. However, for experimental designs in arthroscopic characterization, where adjacent measurement locations create spatially dependent datasets, PLSR is limited due to assumptions on the independence of observations[20,21]. Conforti *et al.* have presented a similar hybrid method based on PLS with LME for assessing spatial variations in soil organic matter[45]. However, since PLS requires both predictors (spectra) and responses (values of tissue properties), it is unsuitable in independent testing scenarios, such as in clinical settings. Hence, PCA-LME was chosen as a regression technique for the present arthroscopic study[22]. The correlations in the independent *in vitro* group for biomechanical properties outperformed the correlations reported in previous study[22], possibly due to a wider spectral region utilized in the current study.

Arthroscopic evaluation of cartilage properties with NIRS has several challenges. Narrow joint spaces restrict access to cartilage surfaces during arthroscopy, potentially explaining the consistent decrease in arthroscopic correlations when compared to *in vitro* results[23]. The main limitation identified in this study was the noisy arthroscopic spectra due to non-optimal probe-cartilage contact. Predicted tissue properties with unclassified spectra resulted in poor correlations, necessitating the application of the kNN classifier to statistically identify and exclude outlying spectra resulting from non-optimal probe contact. This novel application of a classifier-based selection of optimal spectra enhanced the prediction accuracy (Figs. 4 and 5). Furthermore, possible mismatch (despite due diligence) with locations of spectral acquisition during arthroscopy locations and biomechanical measurements may have contributed to weaker correlations. Future studies should focus on improving the arthroscopic spectral acquisition and testing the current prediction models *in vivo*. We acknowledge that the prediction model in this proof-of-concept study would be more generalizable with more diversity in terms of in age and gender. Future studies could employ the protocols developed in Prakash *et al.*[22] and this study to develop a more general cartilage prediction model.

Arthroscopic NIRS could substantially enhance the identification of damaged cartilage by enabling quantitative evaluation of cartilage biomechanical properties. The results advocate employing hybrid multivariate regression models and NIRS in clinical applications. Importantly, the techniques described in the current study can be extended to other spectroscopic evaluations of tissue properties.

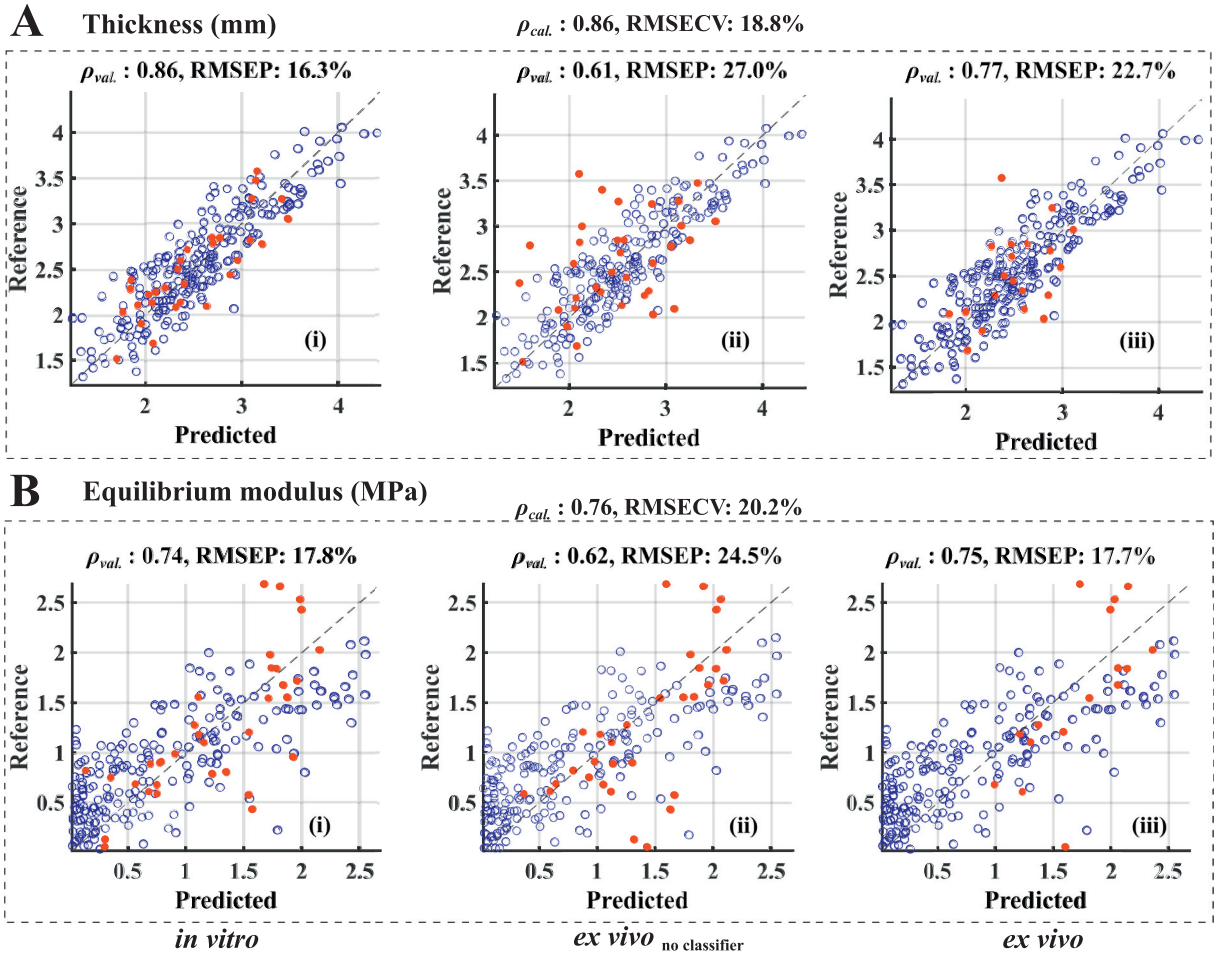

Fig. 5. Predicted vs reference values of cartilage thickness (A) and equilibrium modulus (B) are presented with the Spearman's rank correlation (ρ) and root mean squared error (RMSE) of cross-validation (*RMSECV*) and prediction (*RMSEP*). Calibration data (blue, unfilled) and test set (red, filled) are displayed in all subplots (representative data for 1 iteration). *In vitro* model performance (i), the effect of not using the classifier on *ex vivo* spectra (ii), and using the classifier *ex vivo* spectra (iii) are shown.

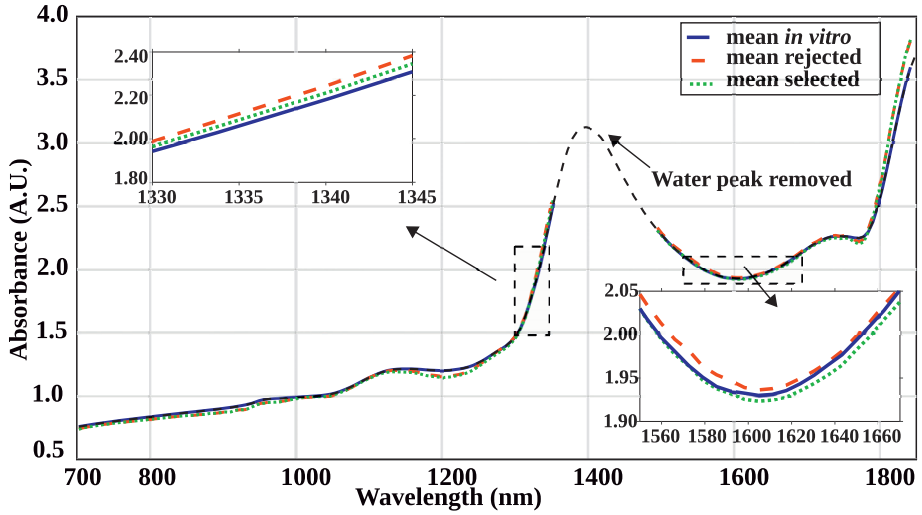

Fig. 6. NIR spectra showing the role of kNN classifier in discriminating *ex vivo* spectra. The inset figures with magnified areas of selected spectral regions show the deviation of spectra relative to the mean *in vitro* spectra.

Author contributions

Prakash, M.: Sample extraction, data acquisition & analysis, protocol design.

Joukainen, A.: Arthroscopic surgery and sample extraction.

Torniainen, J.: Protocol and data analysis.

Honkanen, M.K.M.: Data acquisition and analysis.

Rieppo, L. and **Afara, I.O.:** Study design and supervision of statistical analyses.

Kröger, H and **Töyräs, J.:** Study conception and design.

Sarin, J.K.: Study design and analysis protocol.

All authors contributed to the preparation and approval of the final submitted manuscript.

Conflict of Interest

The authors have no conflicts of interest related to the execution of this study and preparation of the manuscript.

Acknowledgements

Markus Malo, (Ph.D.), Mikko Finnilä (Ph.D.), Tuomas Virén (Ph.D.), Juuso T. J. Honkanen (Ph.D.), Katariina A. H. Myller (M.Sc.) and other members of Biophysics of Bone and Cartilage group, Kuopio, Finland, are acknowledged for assistance during arthroscopies and sample extraction. Sandra Sefa, (M.Sc.) and Ervin Nippolainen (Ph.D.) are acknowledged for assistance with the biomechanical measurements. This study was funded by the Academy of Finland (projects 267551, 2315820 and 269315, University of Eastern Finland), Research Committee of the Kuopio University Hospital Catchment Area for the State Research Funding (project PY210, 5041750, 5041744, 5041772, 5041746, 5041757, 5654149 and 5041778), Kuopio, Finland), Instrumentarium Science Foundation (170033), and The Finnish Foundation for Technology Promotion (8193, 6227).

References

1. Hunziker EB, Quinn TM, Häuselmann H-J. Quantitative structural organization of normal adult human articular cartilage. Osteoarthritis Cartilage 2002;10(7):564–72, https://doi.org/10.1053/joca.2002.0814.
2. Kempson GE, Freeman MA, Swanson SA. Tensile properties of articular cartilage. Nature 1968;220(5172):1127–8, https://doi.org/10.1038/2201127B0.
3. Laasanen MS, Töyräs J, Korhonen RK, Rieppo J, Saarakkala S, Nieminen MT, *et al*. Biomechanical properties of knee articular cartilage. Biorheology 2003;40(1,2,3):133–40.
4. Bader DL, Kempson GE. The short-term compressive properties of adult human articular cartilage. Bio Med Mater Eng 1994;4(3):245–56, https://doi.org/10.3233/BME-1994-4311.
5. Korhonen RK, Laasanen MS, Töyräs J, Lappalainen R, Helminen HJ, Jurvelin JS. Fibril reinforced poroelastic model predicts specifically mechanical behavior of normal, proteoglycan depleted and collagen degraded articular cartilage. J Biomech 2003;36(9):1373–9, https://doi.org/10.1016/S0021-9290(03)00069-1.
6. Mow VC, Fithian DC, Kelly MA. Fundamentals of articular cartilage and meniscus biomechanics. In: Articular Cartilage and Knee Joint Function: Basic Science and Arthroscopy. New York: Raven Press Ltd; 1990:852–70. Raven Press.
7. Lyyra T, Jurvelin J, Pitkänen P, Väätäinen U, Kiviranta I. Indentation instrument for the measurement of cartilage stiffness under arthroscopic control. Med Eng Phys 1995;17(5):395–9, https://doi.org/10.1016/1350-4533(95)97322-G.
8. Korhonen R, Laasanen M, Töyräs J, Rieppo J, Hirvonen J, Helminen H, *et al*. Comparison of the equilibrium response of articular cartilage in unconfined compression, confined compression and indentation. J Biomech 2002;35(7):903–9, https://doi.org/10.1016/S0021-9290(02)00052-0.
9. Buckwalter JA, Mankin HJ. Articular cartilage: degeneration and osteoarthritis, repair, regeneration, and transplantation. Instr Course Lect 1998;47:487–504.
10. Sophia Fox AJ, Bedi A, Rodeo SA. The basic science of articular cartilage: structure, composition, and function. Sport Heal A Multidiscip Approach 2009;1(6):461–8, https://doi.org/10.1177/1941738109350438.
11. Buckwalter JA. Articular cartilage: injuries and potential for healing. J Orthop Sport Phys Ther 1998;28(4):192–202, https://doi.org/10.2519/jospt.1998.28.4.192.
12. Hjelle K, Solheim E, Strand T, Muri R, Brittberg M. Articular cartilage defects in 1,000 knee arthroscopies. Arthrosc J Arthrosc Relat Surg 2002;18(7):730–4, https://doi.org/10.1053/jars.2002.32839.
13. Brismar BH, Wredmark T, Movin T, Leanderson J, Svensson O. Observer reliability in the arthroscopic classification of osteoarthritis of the knee. J Bone Jt Surg 2002;84(1):42–7, https://doi.org/10.1302/0301-620X.84B1.11660.
14. Liukkonen J, Hirvasniemi J, Joukainen A, Penttilä P, Virén T, Saarakkala S, *et al*. Arthroscopic ultrasound technique for simultaneous quantitative assessment of articular cartilage and subchondral bone: an in vitro and in vivo feasibility study. Ultrasound Med Biol 2013;39(8):1460–8, https://doi.org/10.1016/j.ultrasmedbio.2013.03.026.
15. Ayral X. Diagnostic and quantitative arthroscopy: quantitative arthroscopy. Bailliere's Clin Rheumatol 1996;10(3):477–94, https://doi.org/10.1016/S0950-3579(96)80045-8.
16. Rieppo L, Töyräs J, Saarakkala S. Vibrational spectroscopy of articular cartilage. Appl Spectrosc Rev 2017;52(3):249–66, https://doi.org/10.1080/05704928.2016.1226182.
17. Afara IO, Prasadam I, Moody H, Crawford R, Xiao Y, Oloyede A. Near infrared spectroscopy for rapid determination of mankin score components: a potential tool for quantitative characterization of articular cartilage at surgery. Arthrosc J Arthrosc Relat Surg 2014;30(9):1146–55, https://doi.org/10.1016/j.arthro.2014.04.097.
18. Sarin JK, Amissah M, Brommer H, Argüelles D, Töyräs J, Afara IO. Near infrared spectroscopic mapping of functional properties of equine articular cartilage. Ann Biomed Eng 2016;44(11):3335–45, https://doi.org/10.1007/s10439-016-1659-6.
19. Prakash M, Sarin JK, Rieppo L, Afara IO, Töyräs J. Optimal regression method for near-infrared spectroscopic evaluation of articular cartilage. Appl Spectrosc 2017;71(10):2253–62, https://doi.org/10.1177/0003702817726766.
20. Singer M, Krivobokova T, Munk A, de Groot B. Partial least squares for dependent data. Biometrika 2016;103(2):351–62, https://doi.org/10.1093/biomet/asw010.
21. Ranstam J. Repeated measurements, bilateral observations and pseudoreplicates, why does it matter? Osteoarthritis Cartilage 2012;20(6):473–5, https://doi.org/10.1016/J.JOCA.2012.02.011.
22. Prakash M, Sarin JK, Rieppo L, Afara IO, Töyräs J. Accounting for spatial dependency in multivariate spectroscopic data. Chemometr Intell Lab Syst 2018;182:166–71, https://doi.org/10.1016/j.chemolab.2018.09.010.
23. Sarin JK, te Moller NCR, Mancini IAD, Brommer H, Visser J, Malda J, *et al*. Arthroscopic near infrared spectroscopy enables simultaneous quantitative evaluation of articular cartilage and subchondral bone in vivo. Sci Rep 2018;8(1):13409, https://doi.org/10.1038/s41598-018-31670-5.

24. Brittberg M, Winalski CS. Evaluation of cartilage injuries and repair. J Bone Jt Surgery-American 2003;85:58–69, https://doi.org/10.2106/00004623-200300002-00008.
25. Rinnan Å, F van den Berg, Engelsen SB. Review of the most common pre-processing techniques for near-infrared spectra. TrAC Trends Anal Chem (Reference Ed) 2009;28(10):1201–22, https://doi.org/10.1016/j.trac.2009.07.007.
26. Prakash M, Joukainen A, Sarin JK, Rieppo L, Afara IO, Töyräs J. Near-infrared spectroscopy based arthroscopic evaluation of human knee joint cartilage, through automated selection of an anatomically specific regression model. In: Biophotonics Congress: Biomedical Optics Congress 2018 (Microscopy/Translational/Brain/OTS). Vol Part F90-O. Washington, D.C.: OSA; 2018, https://doi.org/10.1364/OTS.2018.OF4D.3. OF4D.3.
27. Fix E, Hodges JL. Discriminatory analysis. Nonparametric discrimination: consistency properties. Int Stat Rev/Rev Int Stat. 1989;57(3):238, https://doi.org/10.2307/1403797.
28. Nakagawa S, Schielzeth H. A general and simple method for obtaining R 2 from generalized linear mixed-effects models. In: O'Hara RB, Ed. Methods Ecol Evol 2013;4(2):133–42, https://doi.org/10.1111/j.2041-210x.2012.00261.x.
29. Hauke J, Kossowski T. Comparison of values of Pearson's and spearman's correlation coefficients on the same sets of data. Quaest Geogr 2011;30(2):87–93, https://doi.org/10.2478/v10117-011-0021-1.
30. Bellon-Maurel V, Fernandez-Ahumada E, Palagos B, Roger J-M, McBratney A. Critical review of chemometric indicators commonly used for assessing the quality of the prediction of soil attributes by NIR spectroscopy. TrAC Trends Anal Chem (Reference Ed) 2010;29(9):1073–81, https://doi.org/10.1016/J.TRAC.2010.05.006.
31. Jia X, Chen S, Yang Y, Zhou L, Yu W, Shi Z. Organic carbon prediction in soil cores using VNIR and MIR techniques in an alpine landscape. Sci Rep 2017;7(1):2144, https://doi.org/10.1038/s41598-017-02061-z.
32. Spahn G, Klinger HM, Hofmann GO. How valid is the arthroscopic diagnosis of cartilage lesions? Results of an opinion survey among highly experienced arthroscopic surgeons. Arch Orthop Trauma Surg 2009;129(8):1117–21, https://doi.org/10.1007/s00402-009-0868-y.
33. Hofmann GO, Marticke J, Grossstück R, Hoffmann M, Lange M, Plettenberg HKW, *et al*. Detection and evaluation of initial cartilage pathology in man: a comparison between MRT, arthroscopy and near-infrared spectroscopy (NIR) in their relation to initial knee pain. Pathophysiology 2010;17(1):1–8, https://doi.org/10.1016/j.pathophys.2009.04.001.
34. Spahn G, Felmet G, Hofmann GO. Traumatic and degenerative cartilage lesions: arthroscopic differentiation using near-infrared spectroscopy (NIRS). Arch Orthop Trauma Surg 2013;133(7):997–1002, https://doi.org/10.1007/s00402-013-1747-0.
35. Afara I, Singh S, Oloyede A. Application of near infrared (NIR) spectroscopy for determining the thickness of articular cartilage. Med Eng Phys 2013;35(1):88–95, https://doi.org/10.1016/j.medengphy.2012.04.003.
36. Marticke JK, Hösselbarth A, Hoffmeier KL, Marintschev I, Otto S, Lange M, *et al*. How do visual, spectroscopic and biomechanical changes of cartilage correlate in osteoarthritic knee joints? Clin Biomech 2010;25(4):332–40, https://doi.org/10.1016/j.clinbiomech.2009.12.008.
37. Afara IO, Hauta-Kasari M, Jurvelin JS, Oloyede A, Töyräs J. Optical absorption spectra of human articular cartilage correlate with biomechanical properties, histological score and biochemical composition. Physiol Meas 2015;36(9):1913–28, https://doi.org/10.1088/0967-3334/36/9/1913.
38. Buckwalter JA, Mankin HJ. Articular cartilage - tissue design and chondrocyte-matrix interactions. J Bone Jt Surg 1998;47:600–11, https://doi.org/.
39. Padalkar MV, Pleshko N. Wavelength-dependent penetration depth of near infrared radiation into cartilage. Analyst 2015;140(7):2093–100, https://doi.org/10.1039/C4AN01987C.
40. Cugmas B, Bregar M, Bürmen M, Pernuš F, Likar B. Impact of contact pressure–induced spectral changes on soft-tissue classification in diffuse reflectance spectroscopy: problems and solutions. J Biomed Opt 2014;19(3), 037002, https://doi.org/10.1117/1.JBO.19.3.037002.
41. Reif R, Amorosino MS, Calabro KW, A'Amar O, Singh SK, Bigio IJ. Analysis of changes in reflectance measurements on biological tissues subjected to different probe pressures. J Biomed Opt 2008;13(1), 010502, https://doi.org/10.1117/1.2870115.
42. Chen W, Liu R, Xu K, Wang RK. Influence of contact state on NIR diffuse reflectance spectroscopy in vivo. J Phys D Appl Phys 2005;38(15):2691–5, https://doi.org/10.1088/0022-3727/38/15/022.
43. Afara IO, Florea C, Olumegbon IA, Eneh CT, Malo MKH, Korhonen RK, *et al*. Characterizing human subchondral bone properties using near-infrared (NIR) spectroscopy. Sci Rep 2018;8(1):9733, https://doi.org/10.1038/s41598-018-27786-3.
44. Baykal D, Irrechukwu O, Lin PC, Fritton K, Spencer RG, Pleshko N. Nondestructive assessment of engineered cartilage constructs using near-infrared spectroscopy. Appl Spectrosc 2010;64(10):1160–6, https://doi.org/10.1366/000370210792973604.
45. Conforti M, Castrignanò A, Robustelli G, Scarciglia F, Stelluti M, Buttafuoco G. Laboratory-based Vis–NIR spectroscopy and partial least square regression with spatially correlated errors for predicting spatial variation of soil organic matter content. Catena 2015;124:60–7, https://doi.org/10.1016/j.catena.2014.09.004.